Materiales de Construcción
Vol. 73, Issue 351, July-September 2023, e321
ISSN-L: 0465-2746
https://doi.org/10.3989/mc.2023.309922

Fresh, hardened and durability properties of sodium carbonate-activated Algerian slag exposed to sulfate and acid attacks

R. Kahlouche [a] ✉, A. Badaoui [a], M. Criado [b]

a. LTPiTE research laboratory, Ecole Nationale Supérieure des Travaux Publics, (Algiers, Algeria)
b. Instituto de Ciencias de la Construcción Eduardo Torroja, IETcc-CSIC, (Madrid, Spain)
✉: r.kahlouche@enstp.edu.dz

Received 20 October 2022
Accepted 14 March 2023
Available on line 10 August 2023

ABSTRACT: This paper investigates the use of Na_2CO_3 as an alkaline activator on the durability of the alkali-activated slag (AAS) mortar toward sulfates and acids. The behavior of this binder in these aggressive environments is compared to those of slags activated with Na_2SiO_3 and NaOH. In addition, the setting times, workabilities, mechanical properties and drying shrinkage were evaluated. The AAS had superior workabilities, faster setting times and higher shrinkage rates than the Portland cement (PC). Increases in the activator dosages had positive effects on the mechanical strengths of the materials. Na_2SiO_3 was the best activator in terms of strength development, but it led to much higher shrinkage. The AAS showed less expansion and lower weight losses than the PC when exposed to sulfate and acids, respectively. The Na_2CO_3-AAS exhibited less shrinkage and higher resistance to sulfuric acid than the other activators, but the mechanical strength seen at early ages was low.

KEY WORDS: Alkali-activated slag; Sodium carbonate; Mechanical strength; Drying shrinkage; Sulfate resistance; Acid attack.

Citation/Citar como: Kahlouche, R.; Badaoui, A.; Criado M. (2023) Fresh, hardened and durability properties of sodium carbonate-activated Algerian slag exposed to sulfate and acid attacks. Mater. Construcc. 73 [351], e321. https://doi.org/10.3989/mc.2023.309922.

RESUMEN: *Propiedades en estado fresco, endurecido y de durabilidad de escoria argelina activada con carbonato sódico frente a los ataques por sulfato y ácido.* En este trabajo se investiga el efecto de usar Na_2CO_3 como activador sobre la durabilidad presentada por los morteros de escoria activados alcalinamente (AAS) frente a los ataques por sulfato y por ácido. Los resultados muestran que las AAS presentan una mayor trabajabilidad, tiempo de fraguado rápido y una alta retracción comparados con la muestra de cemento Portland (PC). El aumento de la dosis del activador tiene un efecto positivo en la resistencia mecánica. El mortero de AAS-Na_2SiO_3 es el mejor activador en términos de desarrollo de resistencias, pero presenta una retracción más alta. La expansión de AAS cuando es expuesto a Na_2SO_4 y la pérdida de peso experimentada en ambos ácidos es menor que aquellas presentadas por el PC. El mortero de AAS-Na_2CO_3 tiene una baja retracción y una alta resistencia al H_2SO_4 en comparación con los AAS-Na_2SiO_3 y NaOH, aunque su resistencia mecánica es baja a edad temprana.

PALABRAS CLAVE: Escoria activada alcalinamente; Carbonato sódico; Resistencia mecánica; Retracción por secado; Resistencia a los sulfatos; Ataque ácido.

1. INTRODUCTION

The increased world population has generated significant energy consumption in all areas of industry, which has contributed to the global climate changes linked to gas emissions. The production of Portland cement (PC) results in the emission of approximately 700 kg of carbon dioxide (CO_2) into the atmosphere for every ton of PC produced (1). The cement industry accounts for approximately 7% of all global emissions, with a heat demand of 3500 to 5000 MJ per ton of clinker (2). This environmental impact makes the use of alkali-activated binders very interesting, and these are produced through the reactions of aluminosilicates such as slag with an alkaline activator. This represents a good option for reducing CO_2 emissions. Commercialization of the alkali-activated binders would require a detailed understanding of the chemical properties of these binders, such as the setting times, workabilities, hydration kinetics and durabilities (3). The reactivity and mechanical strength development of the slag depend on its chemical composition, fineness, curing temperature, and type and concentration of the activator (4-8). Moreover, slag, which is a byproduct of the iron industry, has variable chemical compositions, and these depend mainly on the raw material and the industrial process used (9). The hydration of slag in water is slow, and a glassy shell that forms around the slag grain prevents advanced hydration (10); therefore, it is necessary to use an alkaline activating agent such as sodium hydroxide or sodium silicate to promote the reaction. The use of an alkaline activator accelerates dissolution of the silica and alumina ions by breaking the Si-O and Al-O bonds and leads to precipitation of the hydrates (11-14). Bai et al. (15) show that the initial pH plays an important role in the dissolution of slag and the development of the initial hydration products, but advanced hydration depends primarily on the reaction of the Ca^{2+} dissolved from the slag with the activator anion.

Traditional alkaline activators such as NaOH and Na_2SiO_3 are normally used, but they have several limitations, including their corrosive natures, energy-intensive production methods, high costs and CO_2 emission levels, and complex production systems because they are not available in nature (16, 17). Na_2CO_3 has a negligible carbon footprint, is abundant in nature, is easy to handle, is potentially beneficial in terms of health and safety, has proven effective in the activation process and can be utilized as an alkaline activator (18). However, its use with AASs leads to low mechanical strengths at early stages and fast setting times. In general, the behavior of the AAS depends mainly on the nature and dosage of the activator, the curing conditions and the chemical composition of the slag. These parameters have prevented commercialization and universal formulation of these binders, which need to be optimized.

Alkali-activated slag materials prepared from sodium hydroxide and/or sodium silicate are also characterized by higher mechanical strengths, faster setting times and reduced susceptibilities to chemical attack than PC (19-21). However, shrinkage is the main problem limiting their use instead of PC; this higher shrinkage results from the nature of the gel formed and the higher mesopore content in the AAS, which tend to result in more significant shrinkage compared to PC (22, 23). In addition, there are few studies in the literature that evaluated the durabilities of sodium carbonate-activated slags exposed to acids and sulfates, and more research is needed.

Acid resistance is important because concrete structures can be exposed to aggressive environments during mineral processing, mining, and other industrial processes and experience deterioration. The action of acids on cement paste involves attacks on the hardened paste components; this leads to conversions of all calcium compounds in the unreacted residue and hydration products to form calcium salts of the attacking acid, which destroys the binding capacity of the hardened cement (19). Siad et al. (24) reported that portlandite ($Ca(OH)_2$) dissolved completely in a 5% sulfuric acid solution, while calcium silicate hydrate gel underwent progressive decalcification and the formation of other hydrates. A binder's resistance to acid attack can be evaluated by measuring the weight loss, compressive strength, and corroded depth. Aliques-Granero et al. (25) reported increases in the masses and expansion degrees of AAS samples activated by Na_2SiO_3 with increasing dosage (3% and 5% wt.) of the sulfuric acid solution, and the degradation appeared as cracks on the cube edges and extended toward the centers of the specimens, but no erosion-like phenomena were observed. In another study (26), NaOH was used to activate slag, and more strength reduction was observed for treatment with sulfuric acid (5% H_2SO_4) than with hydrochloric acid (5% HCl). The high loss of strength in sulfuric acid was attributed to deterioration of the concrete due to the formation of expansive gypsum from the calcium ions in the slags and the sulfate ions in the acid solutions. In contrast, when the AAS mortars were exposed to hydrochloric acid, calcium chloride ($CaCl_2$) was formed in smaller amounts, the salt hardly leached out of the concrete through the pores, and minimal deterioration resulted. Pereira et al. (27) demonstrated that activation of the slag by Na_2SiO_3 and NaOH provided lower mass losses in 0.5 M hydrochloric acid than those seen for PC, and this lower mass loss of the alkali-activated binder was related to the absence of portlandite and the lower Ca/Si ratio relative to that in PC.

The degradation processes of cementitious materials in the presence of sulfates can result in expansion, cracking and spalling. The degradation of cement by sulfate occurs through the formation of expansive products, including gypsum ($CaSO_4 \cdot 2H_2O$)

and ettringite (AFt, $3CaO{\cdot}Al_2O_3{\cdot}3CaSO_4{\cdot}32H_2O$). Portlandite reacts with sulfates to form gypsum, and ettringite forms from a monosulfate (AFm, $3CaO{\cdot}Al_2O_3{\cdot}CaSO_4{\cdot}12H_2O$) and sulfate ions. These products occupy larger volumes than the compounds they replace (28-30). Moreover, crystallization of these products in highly saturated pores or in mesopores generates damaging pressures, causing damage to the material (31). In the literature, the evaluation of sulfate resistance for AAS is based on the ordinary cement standard ASTM C1012 (32). AAS prepared with NaOH has higher stability in sodium sulfate (5% Na_2SO_4) than in magnesium sulfate (5% $MgSO_4$), and the latter leads to expansion due to the formation of gypsum (33). Several studies (27, 34) have shown that slag specimens activated with Na_2SiO_3 and NaOH showed lower reductions in mechanical strength and expansion than PC specimens in sulfate environments. The low compressive strengths of the PC specimens are due to the formation of expansive products such as gypsum or ettringite. In contrast to the alkali-activated binders, which did not form portlandite, reduced amounts of the expansive products resulted in limited material deterioration. Another study (35) indicated that an AAS paste showed low levels of ettringite formation in Na_2SO_4 solutions, especially when Na_2CO_3 was employed as the alkaline activator; this prevented ettringite formation and led to stronger resistance against sulfate attack. On the other hand, the attack of Na_2CO_3-activated slag paste by a $MgSO_4$ solution was more aggressive than that of a Na_2SO_4 solution, which led to greater degradation and loss of strength due to the formation of gypsum via the reaction between SO_4^{2-} and Ca^{2+} ions and transformation of the C-A-S-H gel into noncementitious and fibrous magnesium aluminosilicate-hydrate (M-A-S-H) gel (36).

The durabilities of AAS materials are mainly related to the hydration products formed, their sizes, and the degrees of porosity. These factors also depend on the curing conditions, nature, and dosage of the activator. In addition, few studies of slag activation by Na_2CO_3 have appeared in the literature, resulting in limited information on the behaviors of Na_2CO_3-activated slags exposed to chemical attack, such as their corrosion depths. This lack of information confirms the need for this work. Therefore, this study was designed aid in the global commercialization of AAS by determining the behavior of Na_2CO_3-activated Algerian slag mortar cured at 95% relative humidity (RH) and 23 °C; these were subjected to aggressive environments, such as sulfates, hydrochloric and sulfuric acids, and the results obtained were compared under the same exposure conditions for slags activated with Na_2SiO_3 and NaOH. For comparative purposes, a similar study was carried out with PC as the reference material. In addition, the effects of activator dosage and the natures and silicate moduli on the properties of fresh and aged samples were evaluated with the setting times, workabilities, mechanical properties and drying shrinkage of the AAS.

2. EXPERIMENTAL PROGRAM

2.1. Materials

Portland cement class CEM I 42.5 R was used as the reference binder. Granulated blast-furnace slag byproduct from the El-Hadjar steel factory (Annaba, Algeria) was used in this study. The chemical composition was determined by X-ray fluorescence (XRF) with a Rigaku ZSX Primus II spectrometer, and the physical properties of the cement and slag are presented in Table 1. The specific surface areas corresponded to the Blaine fineness, which was evaluated according to European standard EN 196-6. The X-ray diffraction patterns of the cement and slag are shown in Figure 1. The PC was composed of 59.63% alite (C_3S), 16.75% belite (C_2S), 7.77% tricalcium aluminate (C_3A), 11.25% tetracalcium aluminoferrite (C_4AF) and 4.60% gypsum ($CaSO_4.2H_2O$). The diffractogram of the raw slag showed a predominantly amorphous halo at approximately 22-38° (2θ) and calcite ($CaCO_3$).

Table 1. Chemical compositions and physical properties of the cement and slag.

Oxide	Cement	Slag
SiO_2 (%)	21.03	41.06
Al_2O_3 (%)	5.17	8.69
Fe_2O_3 (%)	3.61	1.31
CaO (%)	64.01	43.40
MgO (%)	0.78	3.05
SO_3 (%)	2.55	1.22
Na_2O (%)	0.27	0.13
K_2O (%)	0.50	0.98
Loss on ignition (%)	1.22	0.15
Specific Gravity (g/cm³)	3.14	2.93
Blaine Fineness (cm²/g)	3600	3600

2.2. Paste and mortar formulations

Alkali-activated slag binders were produced by activating the slag with liquid sodium silicate (Na_2SiO_3) composed of 27.8 wt% SiO_2, 8.2 wt% Na_2O, 64 wt% H_2O, sodium hydroxide pellets (NaOH, 98% pure) and sodium carbonate (Na_2CO_3, 98% pure). The activation solutions were prepared from three activators with various dosages and silicate moduli ($Ms=SiO_2/Na_2O$). The dosages of Na_2O and Na_2CO_3 were calculated from the slag mass.

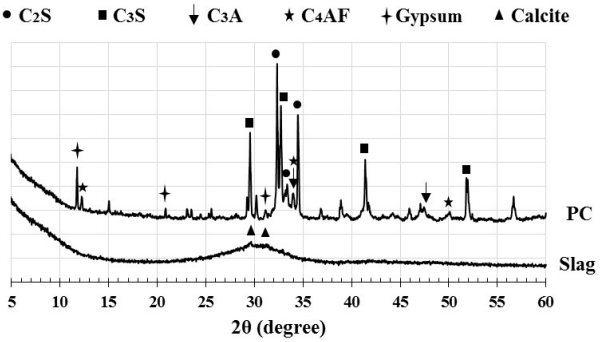

Figure 1. X-ray diffractograms of slag and PC.

The mixing proportions of the AAS binders are presented in Table 2.

Siliceous sand with a 0/3 mm fraction and a fineness modulus of 1.98 was used to produce the mortars. The PC and AAS mortars were prepared according to EN 196-1, with water to binder (W/B) ratios of 0.5 and sand to binder ratios of 3. These ratios required 225 g of water, 450 g of binder, and 1350 g of sand for the final mortar mixture. These masses were kept constant for all mixtures. The binder pastes for the X-ray diffraction (XRD) and thermogravimetric (TG) analyses were prepared with W/B ratios of 0.27. This ratio was selected based on the normal consistencies of the pastes. For the setting time measurements, the pastes were mixed to the normal consistency required by the standard.

2.3. Methods

Initially, the nature and dosage of the alkaline activators and the silicate moduli and their effects on the fresh properties of the alkali-activated samples and the reference sample were evaluated. The workability of the mortar was evaluated with a flow table by measuring the spreading diameter as in the EN 1015-3 standard. The setting times (initial and final) of the pastes were measured with a Vicat apparatus according to EN 196-3. Subsequently, the effects of these variables on the properties of the hardened samples were studied by determining the mechanical strengths and shrinkage. The mortar mixtures were cast into 40×40×160 mm^3 prismatic steel molds and vibrated on a shock table. After demolding, the AAS specimens were stored in a humidity chamber at approximately 23 °C and 95% RH, and in water for the PC specimens, until reaching the ages of the flexural and compressive strength tests. The drying shrinkages of the mortars were measured periodically in the laboratory at 20 °C and 55% RH on 40×40×160 mm^3 prisms for up to 12 months, as specified in EN 12617-4.

After that, according to the mechanical strength results, a sample treated with each activator (sodium carbonate, sodium hydroxide and a mixture of sodium hydroxide and sodium silicate) and the PC paste were characterized by XRD and TG to identify the reaction products. The XRD and TG analyses were performed on powders from the 20×20×20 mm^3 cubic paste samples. The cubes were demolded after 24 hours and cured under 95% RH and 23 °C for the AAS and in water for the PC. At the test age, the cubic pastes were ground into powders. The TG analyses were carried out at 28 days of curing with a DTA-50 Thermal Analyzer by heating approximately 10 mg of the paste powder from 50 to 1000 °C in a nitrogen atmosphere with a heating rate of 20 °C/min. After 28 and 180 days of curing, an ADVANCE A25 D8 X-ray diffractometer was used for the XRD analyses, which were carried out over a range of 5° to 60° (2θ) with a scan rate of 1 s/step and a resolution of 0.05°/step.

Finally, these same four formulations were exposed to sulfates and acids to evaluate their durabilities in these aggressive environments. To evaluate the AAS resistance to sulfate attack, the degrees of expansion were measured for three prismatic mortars measuring 40×40×160 mm^3 for each activator and the reference

Table 2. Mixing proportions of the AAS binders (in g).

Mix	Activators	Dosage	Ms	Slag	Na_2SiO_3	NaOH	Na_2CO_3
M1	Sodium Silicate & Sodium Hydroxide	7% Na_2O	0	450	0	40.5	0
M2		4% Na_2O	0.5	450	33	18.7	0
M3		6% Na_2O	0.5	450	49.4	28.1	0
M4		8% Na_2O	0.5	450	66	37.4	0
M5		6% Na_2O	0.75	450	74.1	24.7	0
M6		6% Na_2O	1	450	98.8	21.3	0
M7	Sodium Carbonate	9% Na_2CO_3 (5.26% Na_2O)	0	450	0	0	40.5
M8		15% Na_2CO_3 (8.77% Na_2O)	0	450	0	0	67.5

PC mortar. At 28 days of curing, the samples were immersed in sodium sulfate solutions (5% Na_2SO_4) for 12 months. The lengths were measured every 15 days. The sodium sulfate solution was renewed each month, and the volumes were four times the specimen's volume. On the other hand, the acid attack resistance was evaluated from the weight losses of 40×40×160 mm^3 prismatic specimens over 12 months. After 28 days of curing, three specimens of the mortar were immersed in 3% HCl and 3% H_2SO_4. The acid solution volumes were four times the volume of immersed specimen, and the acid was refreshed each month. The specimens were extracted from the solution monthly, rinsed three times with tap water, blotted with a paper towel, and left to dry at 20 ± 3 °C and 50% RH for 30 min before weighing. After one year of exposure, deterioration of the mortar was determined visually by observing changes in the outer layer of the mortar specimen and by measuring the cross section of the undamaged core after splitting each specimen into two parts to determine the corrosion depth.

Some of the data presented in this study for the reference cement (PC) and the NaOH-activated slag (M1) were from the work of Kahlouche et al. (37).

3. RESULTS

3.1. Effects of the activator nature and dosage and the silicate modulus on the fresh properties of the AAS pastes and mortars

3.1.1. Workability

The flowabilities of the fresh mortars are given in Figure 2; most of the AAS mortars present higher workabilities than the PC mortar. This high workability for the AAS was mainly attributed to the plasticizing effects of the activators. The workability was reduced with increasing Na_2O content in the activating solution. In contrast, increases in the silicate modulus significantly improved the workability. Activation of the slag by NaOH and Na_2CO_3 led to lower workabilities compared to that seen for sodium silicate.

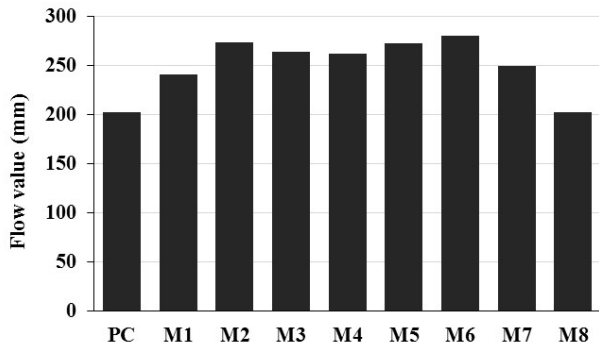

Figure 2. Flow values of the mortars.

3.1.2. Setting time

Figure 3 illustrates the setting times (initial and final) of the different binder pastes. The AAS pastes has shorter setting times than the PC paste. For a silicate modulus of 0.5 (the M2, M3 and M4 samples), increases in the Na_2O dosage significantly reduced the setting times of the binder. The same behavior was seen for the Na_2CO_3-activated slag samples, and increases in the Na_2O dosage also led to reductions in the setting times, which is clearly observed for the values obtained for the M7 and M8 samples. On the other hand, the setting times for the M3, M5 and M6 samples made with 6% Na_2O increased with higher silicate moduli.

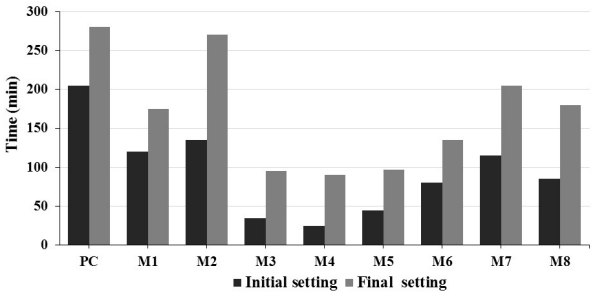

Figure 3. Initial and final setting times of the binders.

3.2. Nature and dosage of activator and silicate modulus and their effects on the properties of the hardened AAS mortars

3.2.1. Mechanical strengths

The compressive strengths of the PC and AAS mortars are given in Table 3. These results showed increases in the strength of all binders with aging; this favored precipitation of the gel, which was responsible for the mechanical development of the material. The Na_2SiO_3-activated slag mortar developed a higher strength compared than the mortars activated with the other activators. The strength of the M6 sample even exceeded that obtained for the PC and represented an increase of 32% after 28 days compared to the PC. Greater compressive strengths also resulted from a high silicate modulus, such as Ms values of 0.75 and 1 (M5 and M6 samples) at 28 days, and the strengths were greater by 12% and 38%, respectively, compared to that obtained with an Ms of 0.5 for the M3 sample. In contrast, at early ages, mortars have lower compressive strengths for high moduli. For the mortars with an Ms=0.5, increases in the Na_2O dosage (6% and 8%, M3 and M4 samples) improved the compressive strengths by 53% and 58% compared to the mortar of the M2 sample treated with 4% Na_2O at 28 days. In addition, the strengths of the mortars activated with this alkaline solution reached more than

90% of their final values at 28 days. On the other hand, the slag mortars activated with NaOH developed the lowest compressive strengths after 28 days, and they were 64% lower than that obtained for the PC mortar. With regard to activation of the slag mortar by Na_2CO_3, it developed very low strengths in the first stages. From 28 days, the strength increased significantly but remained lower than that of the PC mortar. It was also observed that increasing the Na_2O dosage improved the compressive strengths at any age for the M7 and M8 samples.

The flexural strengths of the PC and AAS mortars are also given in Table 3. These results showed that the strengths for the different types of binders increased with age. Activation of the slag mortar by sodium silicate provided flexural strengths lower than that of the PC mortar at 2 days, but the differences tended to equalize over time or in certain cases even exceed these values. The mortar with a 6% Na_2O dosage and an Ms=0.5 (M3 sample) had the highest strength. The variations in the Na_2O dosages and Ms values for the Na_2SiO_3 activator had no remarkable effect on the flexural strengths, and no correlation was found between the evolutions of the flexural strengths and compressive strengths for the different Ms and Na_2O dosages. For the sodium hydroxide-activated slag mortar, the flexural strengths remained lower than that of the PC mortar. Activation of the slag mortar by sodium carbonate did not generate flexural strength during the first stage. However, with increasing activator dosage, the strength increased and became similar to that of the PC mortar at advanced ages.

3.2.2 Drying shrinkage

The drying shrinkage of the PC and AAS mortars is illustrated in Figure 4. The shrinkage values increased with age for all mortar types, but after aging for 56 days, these values remained approximately constant. The AAS mortars showed more shrinkage than the PC mortar. In addition, the slag activated with sodium silicate showed more shrinkage than the slags activated with sodium hydroxide and sodium carbonate. The shrinkage values of the mortars made with 6% Na_2O (samples M3, M5 and M6) significantly increased with increasing silicate moduli, and they increased faster and reached 52%, 82% and 83% at 7 days for the final shrinkage values for moduli of 0.5, 0.75 and 1, respectively. Moreover, for the mortars with Ms=0.5 and 4%, 6% and 8% Na_2O dosages (M2, M3 and M4 samples), the shrinkage values increased by 3, 5 and 6 times, respectively, compared to that of the PC mortar. The NaOH-activated slag mortar exhibited slightly higher shrinkage than the PC mortar; this shrinkage value was the lowest of all values obtained, independent of the alkaline activator employed. It was also seen that increases in the Na_2CO_3 activator dosage (M7 and M8 samples) did not have considerable effects on the shrinkage, except for a slight reduction.

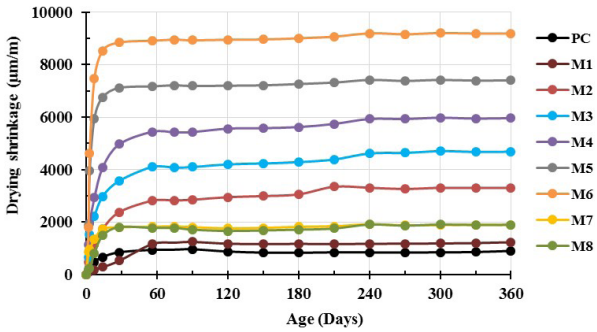

Figure 4. Drying shrinkage levels of the different mortars.

3.3. Characterization of the AAS pastes

In light of the results of the mechanical strengths, the study was extended by choosing one dosage for each activator, depending on the binders that devel-

Table 3. Compressive and flexural strengths of the mortars at different ages.

Mortar type	Compressive strength (MPa)				Flexural strength (MPa)			
	2-Days	7-Days	28-Days	90-Days	2-Days	7-Days	28-Days	90-Days
PC	23.1 ± 0.3	35.4 ± 1.1	44.6 ± 1.1	51.8 ± 1.3	5.1 ± 0.2	6.5 ± 0.1	7.0 ± 0.2	7.4 ± 0.3
M1	5.7 ± 0.1	10.9 ± 0.2	15.8 ± 0.3	21.9 ± 0.6	2.7 ± 0.1	4.5 ± 0.1	4.8 ± 0.1	5.4 ± 0.2
M2	7.7 ± 0.3	15.9 ± 0.4	27.8 ± 0.0	30.4 ± 0.6	1.9 ± 0.3	3.1 ± 0.2	6.9 ± 0.1	7.5 ± 0.1
M3	12.1 ± 1.0	25.3 ± 0.3	42.8 ± 0.3	47.1 ± 1.0	4.0 ± 0.1	8.0 ± 0.1	10.0 ± 0.1	10.5 ± 0.4
M4	13.4 ± 0.4	32.2 ± 1.0	44.0 ± 0.5	49.3 ± 2.3	4.2 ± 0.1	7.3 ± 0.2	7.3 ± 0.3	7.7 ± 0.3
M5	6.6 ± 0.1	29.1 ± 1.5	48.1 ± 1.4	47.4 ± 1.3	2.1 ± 0.1	6.0 ± 0.1	9.0 ± 0.3	9.2 ± .2
M6	8.0 ± 0.1	37.0 ± 2.0	59.1 ± 0.7	59.9 ± 3.4	2.9 ± 0.0	7.0 ± 0.2	8.0 ± 0.0	8.9 ±0.2
M7	0.5 ± 0.0	1.1 ± 0.1	20.7 ± 0.7	29.3 ± 1.3	0.0 ± 0.0	0.0 ± 0.0	4.1 ± 0.3	4.4 ± 0.1
M8	1.4 ± 0.1	3.7 ± 0.2	40.0 ± 2.2	41.3 ± 1.1	0.0 ± 0.0	0.9 ± 0.0	6.3 ± 0.4	6.6 ± 0.2

oped the greater mechanical strengths and taking into account the economic factors. The samples selected were M1, M3, M8 and PC, which were characterized to identify the reaction products.

3.3.1. XRD analyses

Figure 5 illustrates the XRD patterns determined for the PC and AAS pastes (M1, M3 and M8) after 28 and 180 days of hydration. The data show the presence of C-S-H gel, portlandite, ettringite and calcite in the PC paste cured for 28 days. The main reaction product from AAS hydration was C-S-H rich in Al; other crystalline phases were also detected, and their natures depended on the alkaline activator, stratlingite (C_2ASH_8) and hydrotalcite ($Mg_6Al_2CO_3(OH)_{16}•4H_2O$) in NaOH-activated slag paste (M1) and gaylussite ($Na_2Ca(CO_3)_2•5H_2O$) in the Na_2CO_3-activated slag paste (M8). In the diffractogram for the slag paste activated with Na_2SiO_3 (M3), no other crystalline phase was detected. Increased aging did not affect the diffraction peak intensities of the phases formed in the slag samples activated by Na_2SiO_3 and NaOH. In contrast, in the sample activated by Na_2CO_3, the diffractogram presented increases in the intensities of the diffraction peaks for C-A-S-H and gaylussite, indicating progression of the hydration reaction. The XRD patterns confirmed that the different hydration products were already formed at 28 days.

3.3.2. TG/DTG analyses

The TG/DTG curves of the AAS and PC pastes aged for 28 days are presented in Figure 6. For the TG curves, the total weight losses of the samples were 19.7%, 14.3%, 17.7% and 15.6% for PC, M1, M3 and M8, respectively. As shown in Figure 6, most of the weight loss occurred between 50 °C and 250 °C, and up to 100 °C, the mass losses corresponded to free water for all binders and gaylussite for the Na_2CO_3-activated slag (38). The AAS presented a peak at approximately 120 °C that corresponded to dehydration of the C-(A)-S-H gels in the pastes. The mass loss at 350 °C for the NaOH-activated slag was attributed to the decomposition of hydrotalcite (4). Finally, for the temperature range 500-800 °C, the weight losses were due to decarbonation of the carbonate-containing phase (39). For the PC sample, the DTG curve showed three main peaks: the first peak located below 150 °C corresponded to dehydration of the C-S-H gel and ettringite, the second peak between 450-550 °C was attributed to the dehydration of portlandite, and the third peak corresponded to the decarbonation of calcite at approximately 550 to 800 °C (1, 33). The exothermic peaks for different weight loss percentages occurring at different temperatures confirmed the formation of distinct compounds according to the nature of the binder and the alkaline activator, as previously observed by XRD.

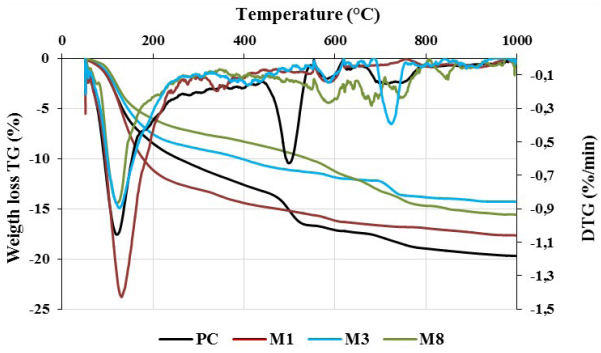

Figure 6. TG/DTG data for the AAS and PC pastes after 28 days of hydration.

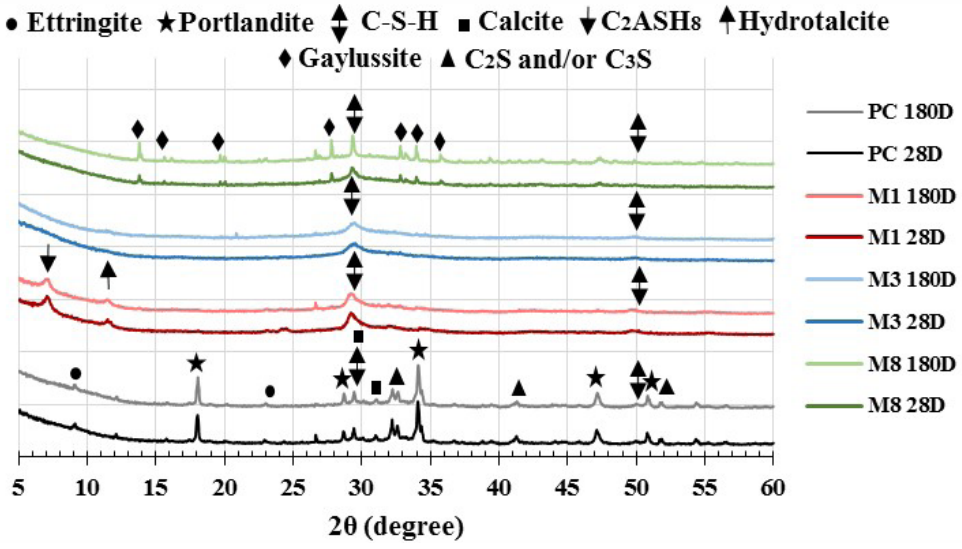

Figure 5. X-ray diffraction diagrams of the cement pastes aged for 28 and 180 days.

3.4. Durabilities of the AAS mortars exposed to sulfates and acid

The previous four samples (M1, M3, M8 and PC) were exposed to sulfate and acid to evaluate their durabilities in these aggressive environments.

3.4.1. Sulfate attack

Figure 7 presents data for the expansion of the PC and AAS (M1, M3 and M8) mortars immersed in sodium sulfate (5% Na_2SO_4) for 12 months. The results showed that expansion of the PC mortar increased with increasing immersion time, which represented the largest mortar expansion, 0.54%, seen at 12 months. Fast acceleration of the expansion was observed from 8 months forward. On the other hand, the AAS mortars presented less expansion that stabilized at values less than 0.03% after 5 months. This represented 95%, 97% and 99% reductions in the amounts of expansion for M1, M3 and M8 at 12 months, respectively, compared to that of the PC mortar. Upon visual inspection, deteriorated areas appeared in the PC mortar after 4 months of exposure, and fine cracks at the edges and spalling at the corners of the specimens were observed, principally due to expansion. These cracks increased with age. For the AAS mortars, no signs of deterioration were seen until 12 months of immersion in a sodium sulfate solution.

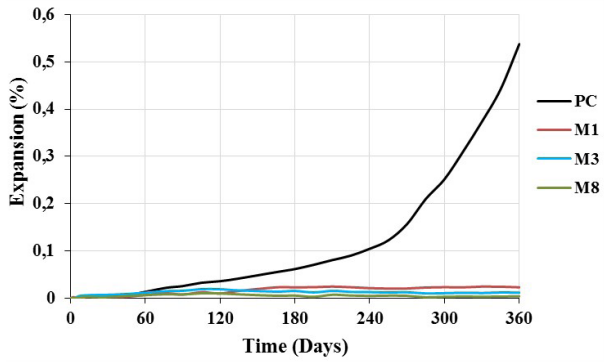

Figure 7. Expansion of the mortars immersed in sodium sulfate solutions.

3.4.2. Acid attack

Figure 8 presents the mass losses of the PC and AAS (M1, M3 and M8) mortars immersed in 3% HCl and 3% H_2SO_4 solutions for 12 months. The PC mortar exhibited greater mass losses than the AAS mortars for immersion in both acids. More weight was lost during exposure to H_2SO_4 than to HCl, with values of 92% and 31%, respectively, after 12 months of exposure. For the M1 and M3 mortars, slight increases in the weights were observed for up to 3 months of exposure to H_2SO_4. At that age, degradation began, and the amounts of mass lost increased with increasing exposure time and reached 44%, 33% and 14% for the M1, M3 and M8 mortars, respectively, at 12 months. For the other specimens immersed in HCl, the mass losses started from the moment of immersion and continued to increase until they reached 14%, 14% and 21% for M1, M3 and M8, respectively, at 12 months.

The slag mortar activated with NaOH (M1) showed lower resistance to sulfuric acid than to hydrochloric acid, and it was one of the most resistant binders to HCl. However, the slag mortar activated by Na_2CO_3 (M8) presented the opposite behavior, and this binder exhibited the highest resistance to H_2SO_4 and a 7% increase in the mass loss due to HCl. When sodium silicate was used as the activator (M3), the degradation behavior (mass loss) observed was the same as that observed for the NaOH-activated slag mortar in HCl. In addition, the weight losses were 54%, 54% and 32% lower for the M1, M3 and M8 samples, respectively, compared to the PC mortar after 12 months of immersion in HCl, and they were 52%, 64% and 85% lower for H_2SO_4 immersion.

Figure 9 shows visible degradation of the mortar specimens after 12 months of immersion in water and both acids. All PC and AAS specimens exposed to HCl acid preserved their dimensions and their prismatic forms and did not exhibit extensive degradation on their external surfaces, except for the loss of small sand grains (see the top of Figure 9). Among the specimens exposed to sulfuric acid (see the bottom of Figure 9), the PC mortar showed severe degrada-

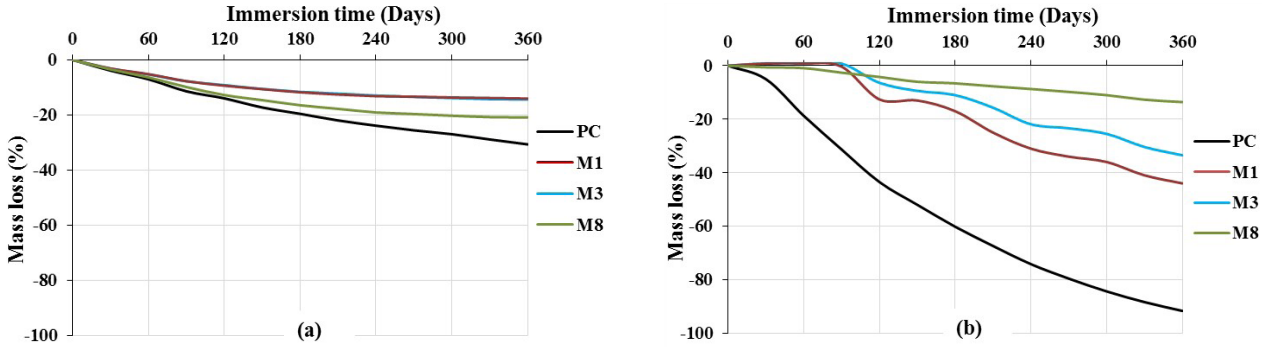

Figure 8. Mass losses of the mortars after immersion in (a) 3% HCl and (b) 3% H_2SO_4.

tion with a reduction in the cross-section of the prism. This reduction was due to dissolution of the binder in the acid-exposed layer, which led to deterioration of the mortar by erosion. Deterioration of the AAS mortar resulted in cracks at the borders of the specimens, which increased with increasing exposure times. The NaOH-activated slag mortar (M1) also showed losses of small parts of the external layers. The Na_2SiO_3-activated slag mortar (M3) showed an increase in the cross-section, which was on average 43×43 mm².

On the other hand, all of the mortars exposed to hydrochloric acid showed complete deterioration of the specimen cores (yellow color), with little loss of mass, and no mechanical strength developed after one year of exposure. For the mortars exposed to sulfuric acid, undamaged cores (the colors were black) were observed with diameters of 10 mm, 18 mm and 22 mm for the mortars M1, M3 and M8, respectively. The core of the reference mortar presented a 12×12 mm² section. The slag activated by sodium carbonate presented the largest undamaged core after immersion in the H_2SO_4 solution and little loss of the outer layer compared to the samples made with the other activators.

4. DISCUSSION

This section presents a scientific discussion of the properties of the AAS in its fresh and hardened states as a function of the nature and dosage of the activator and the silica modulus. These properties were mainly related to reactions of the slag with the components of the alkaline activator.

The high fluidity of the AAS was due to the alkaline activator, which had a plasticizing effect. For example, when sodium silicate was used as an activator, silicate ions were adsorbed onto the surfaces of the slag grains. They adsorbed on the surfaces of the particles, which increased the magnitude of the electric double layer repulsive forces and led to deflocculation of the particles and consequently to increases in the workability (40). The presence of silicate ions in the sodium silicate activator justified the higher fluidity of the AAS compared to those treated with the other activators (NaOH and Na_2CO_3). As for the setting time, the rapid setting of the AAS was attributed to faster dissolution of the slag and formation of more initial hydrates compared to the PC compounds. Particularly for sodium silicate, Palacios et al. (41) detected the formation of a highly polymerized product after only 40 min (sodium aluminosilicate gel and C-A-S-H). It was also mentioned that activation of the slag by NaOH required more time to form C-A-S-H than activation of the slag by Na_2SiO_3. There were initially no silicate species in solution, and the concentrations of silicate and aluminum species, as well as that of calcium ions, slowly increased as the slag dissolved, which explained the faster setting time of the latter.

On the one hand, an increase in the modulus of the silicate led to an increase in the number of silicate ions adsorbed on the particle surface and an increase in the magnitude of the repulsive force, which explains the improvements in workability seen with increasing silicate modulus. In addition, the increased setting time seen with a higher silicate modulus may have been related to the decreased pH of the alkaline solution,

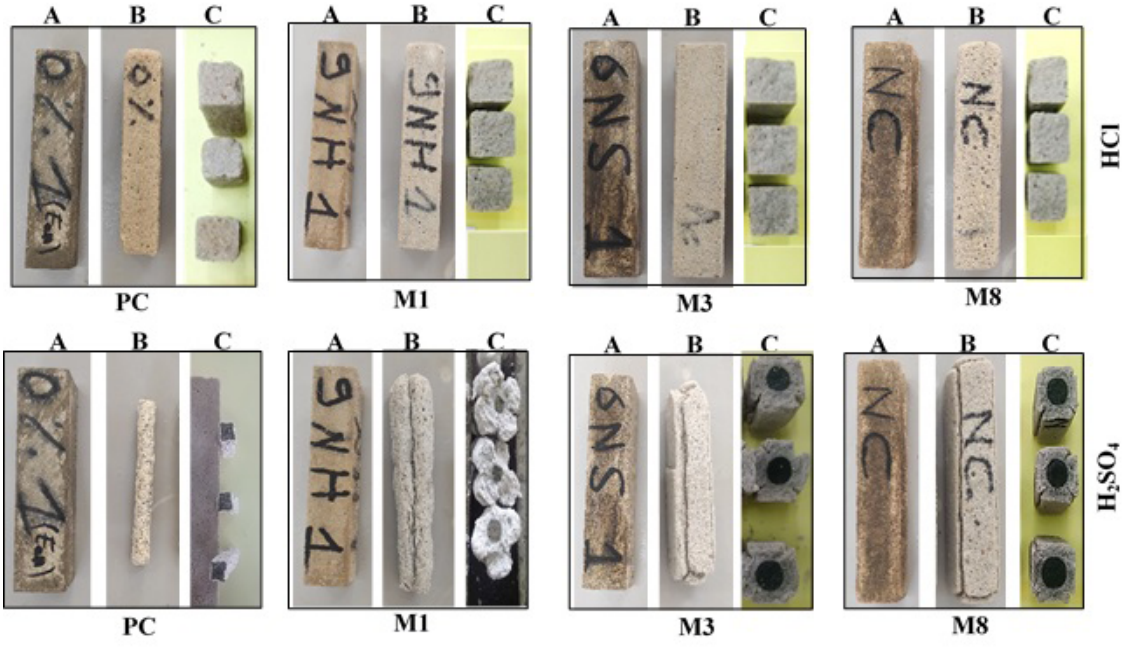

Figure 9. Deterioration of the specimens after 12 months of exposure to 3% HCl and 3% H_2SO_4.
(A: Preserved in water B: Exposed to acid C: Cross section).

which slowed the formation of hydrates and consequently the setting phenomenon. The silicate species were more highly polymerized and reacted slowly with the calcium released from the slag, and the time needed to induce gel formation was elongated (42).

On the other hand, increases in the dosages of the activators containing sodium hydroxide and sodium silicate accelerated dissolution of the slag by breaking the Si-O and Al-O bonds and forming hydration products (C-(A)-S-H) that enhanced the binding properties of the material, which led to reductions of the workabilities and rapid hardening of the specimens with short setting times (43, 44). When Na_2CO_3 was used to activate the slag, the same effect was seen for increased Na_2O dosages, leading to better workability and a reduction in the setting time. Bernal et al. (45) observed that at an early age, the reactions between carbonate (CO_3^{2-}) ions from the Na_2CO_3 with calcium (Ca^{2+}) ions in the slag occurred to form calcite and gaylussite. Moreover, zeolite was also formed from the aluminate and silicate species in the slag due to the sodium from the Na_2CO_3. Subsequently, once the CO_3^{2-} was exhausted, a C-A-S-H gel was formed via a reaction involving calcium, aluminum and silicate dissolved from the slag. Increasing this activator dosage accelerated dissolution of the slag, consumption of the carbonate ions and formation of these hydration products. The diffractograms and the thermogravimetric analyses corroborated the precipitation of these products, gaylussite and carbonates. The presence of gaylussite in the hydration products from Na_2CO_3-activated slags has also been reported in the literature (38, 46, 47).

The main factors affecting the mechanical strength are the hydration products formed during hydration of the binder and the porosity of the material. The different mechanical strengths of the AASs were related to the nature of the hydrates formed with each activator. Taking into account the XRD and TG data for the samples, the main reaction product for all of the samples was the C-A-S-H gel, but the secondary reaction products differed according to the type of activator used. Strantligite and hydrotalcite were detected when sodium hydroxide was employed as the activator, while gaylussite and another carbonate were formed when the slag was activated with sodium carbonate or a mixture of sodium silicate and sodium hydroxide. The low mechanical strength seen at an early age for the slag activated by sodium carbonate was due to the low alkalinity of the activator solution, which delayed the dissolution of slag and hydrate precipitation (48), which enabled the generation of gaylussite and calcite. These phases did not give the high degree of cohesion necessary for the development of high early mechanical strength. At later ages, the increased strengths were due to formation of the C-A-S-H gel, which led to an increased strength (45).

The increased compressive strengths seen with higher silicate moduli were related to the incorporation of silicate anions into the C-A-S-H gel structure, resulting in a decrease in the Ca/Si ratio and thus an improvement in the binding capacity of C-A-S-H (21); the M6 sample exhibited the highest mechanical strength. Additionally, the structures of the samples were densified with higher Ms, leading to lower porosities (21). In addition, over time, more silicate anions were dissolved in the medium, and they were incorporated into the gel structure, refining the matrix and improving the compressive strengths of all samples.

Greater mechanical strength development was observed for increasing activator dosages. This may have been due to the increased alkaline concentrations in the activation solutions. This enabled the dissolution of more calcium and silicate ions in the slag grains and generated more gel, which was responsible for the binding properties; consequently, a higher strength of the system was achieved.

The unremarkable variations in flexural strength with increases in the Na_2O dosage and silicate modulus of the sodium silicate activator may have been related to greater sensitivity of the flexural strength to cracking compared to the compressive strength. In a previous study (21), SEM images showed significant formation of microcracks in the matrix and matrix-aggregate interfaces in samples with high Ms values.

The drying shrinkage resulted from the decreased volume of the material caused by chemical reactions and the exchange of moisture with the environment (23). This occurred through two mechanisms: disjunction pressure, mainly when the material had a very fine porosity, and capillary suction (49). The higher shrinkage of the alkali-activated slag compared to the PC was related to the higher amount of mesopores (with pore diameters between 2.5 and 50 nm) of the AAS, which resulted in higher capillary stresses leading to higher shrinkage (50). In addition, the formation of a calcium silicate gel rich in aluminum during hydration of the sodium silicate-activated slag led to a drying shrinkage higher than that of the PC. This gel had a high water content, which may dry out with water loss (51).

As for the influence of the silicate modulus and the Na_2O dosages for the samples activated with sodium hydroxide or a mixture of sodium hydroxide and sodium silicate, a high Ms and dosage precipitated more C-A-S-H gel, which may explain the increased shrinkage of the specimens. Li et al. (52) found that sodium silicate-activated slag mortar exhibited more drying shrinkage than sodium hydroxide activation. The high shrinkage of the Na_2SiO_3-activated slag mortars was related to the percentage of mesopores. These mortars had higher percentages of mesopores than the slag mortars activated with NaOH, which implied an increase in the water evaporation rate (23). However, when sodium carbonate was employed as the activator, the increased Na_2O dosage had a negligible effect on the shrinkage, which may have been

related to the increased reaction rate, as has been explained previously; this resulted in an increase in the amount of chemically bound water reduced the rate of water evaporation (53).

The durabilities of the AAS mortars exposed to sulfates and acid depended on the nature of the alkaline activator employed and the reaction products formed. For sulfate attack, the expansion of the PC mortar was due to the formation of expansive products (gypsum and ettringite), which exerted great pressure on the pore walls. These expansive products were formed by reactions of the portlandite and AFm phases with sulfate ions (30, 54). The opposite behavior was observed for the AAS mortars, and the low expansion rates of these specimens may have been due to the reaction products formed. The absence of portlandite during hydration of the AAS mortar, independent of the activator (sodium hydroxide, a mixture of sodium hydroxide and sodium silicate, and sodium carbonate) used, resulted in the formation of few expansive products in the sulfate environment and consequently low expansion, as shown by the XRD and TG/DTG analyses. In addition, the AAS mortars exhibited low permeabilities, which enabled less penetration of the aggressive ions compared to the PC mortar (55, 56). The alkaline activator employed did not seem to exert any effect on the durabilities of the AAS mortars during sulfate attack; the damage levels were similar for the three samples.

The AAS mortars exhibited higher resistance than the PC mortar when they were exposed to HCl and H_2SO_4, and the AAS mortars exhibited lower mass losses and larger nondamaged cores than the PC mortar. This high resistance was due to the lower calcium content in the slag, the absence of portlandite indicated by the diffractograms and the TG analysis, and the formation of a C-A-S-H gel with a low Ca/Si ratio. This precluded the precipitation of salts, resulted in low initial permeability and high alkalinity of the pore solution, and provided high stability to an acidic medium (20). The anion of the acid exerted a great influence on the durabilities of the samples because it reacted with the calcium ions of the slag to form a salt of the attacking acid. Greater mass losses occurred for the mortars exposed to H_2SO_4 relative to those exposed to HCl. In the sulfuric acid solution, the reaction between sulfuric acid and the calcium ions formed ample amounts of expansive products such as gypsum, which caused great deterioration of the specimens. In addition, the cracks formed on the edges of these specimens facilitated penetration of the acid ions, which further deteriorated the material due to leaching of the calcium ions (26). The formation of expansive products also resulted in increased cross-sections, as with the M3 mortar. This effect of sulfuric acid on the Na_2SiO_3-activated slag was observed by Aliques-Granero et al. (25). For hydrochloric acid, the chloride ions reacted with the calcium ions and formed small quantities of calcium chloride. This salt was highly soluble and leached out of the concrete through its pores or by creating voids that deteriorated the specimen (26). In these cases, the small amounts of calcium chloride precipitated resulted in less leaching and less deterioration of the samples compared to sulfuric acid exposure.

The specimens activated with sodium hydroxide or a mixture of sodium hydroxide and sodium silicate behaved similarly in the hydrochloric acid, while activation with sodium carbonate provided different results. These samples showed better resistance to sulfuric acid and worse resistance to hydrochloric acid than the other two samples. Ye et al. (35) observed that the carbonate anions suppressed ettringite precipitation from the sodium carbonate-activated slag, and therefore, this sample developed a high resistance toward the aggressive environment. However, the use of the sodium carbonate activator resulted in higher total pore volumes and increased permeabilities of the ions (57), e.g., chloride ions in this case, and therefore enabled increased formation of the chloride salts and further deterioration of the material.

In light of these results, the use of sodium carbonate as the alkaline activator to provide a cementitious material from blast furnace slag is very attractive from the perspectives of environmental and economic factors and material durability. It has the advantages of low drying shrinkage and high resistance to sulfate attack and sulfuric acid, as indicated by the mass losses and deterioration levels of these specimens compared to those made with other activators (sodium silicate and sodium hydroxide), despite the low mechanical strengths at early ages.

5. CONCLUSIONS

This paper presents a study of Algerian slag activated by Na_2CO_3 and its behavior toward aggressive conditions involving sulfates, hydrochloric acid and sulfuric acid, and a comparison is provided with slags activated by Na_2SiO_3 and NaOH. In addition, the effects of dosage and activator type on the workabilities, setting times, mechanical strengths, drying shrinkage levels, and hydration products formed were also evaluated. The main conclusions derived from this investigation were:

- In general, the AAS mortars showed better workabilities than the PC mortars, which improved with increasing silicate modulus. The setting times of the AAS pastes were shorter than those of PC mortars, and increased Na_2O and Na_2CO_3 dosages led to reductions in the setting times.
- The highest compressive strengths were exhibited by Na_2SiO_3-activated slag mortars with high silicate moduli and Na_2O dosages. Greater Na_2CO_3 dosages improved the compressive and flexural strengths, but they remained lower than those of the PC mortar.

- The AAS mortars showed greater shrinkage than the PC mortar. Drying shrinkage of the AAS mortars generally increased with high-modulus silicate and greater Na_2O dosages. The slag mortars activated with NaOH and Na_2CO_3 presented lower drying shrinkage than the slag mortar activated with Na_2SiO_3.
- The XRD and TG/DTG results showed that the C-(A)-S-H gel was the main product of the AAS pastes. However, other crystalline products were formed depending on the type of activator.
- The AAS mortars show high stabilities in sulfate environments and the expansion levels were more than 95% lower than that of the PC mortar.
- Sulfuric acid was more aggressive than hydrochloric acid in terms of mass loss, and the AAS mortars exhibited higher resistance to both acids than the PC mortars. The Na_2SiO_3 and NaOH-activated slags exhibited the best binder resistance to hydrochloric acid.
- Hydrochloric acid attack generated low mass losses but complete deterioration of the specimen core, which exhibited no binding capacity. The opposite behavior occurred upon exposure to sulfuric acid, with a high mass loss and an undamaged specimen core.
- The slag activated by sodium carbonate had the highest resistance to sulfuric acid in terms of mass losses and specimen deterioration but a lower mechanical strength at an early age.

ACKNOWLEDGEMENTS

The authors would like to thank the LTPiTE research laboratory of ENSTP, the COSIDER laboratory, the GICA group (MEFTAH factory), the CRAPC laboratory, the DGRSDT and the Sika Algeria for their support.

AUTHOR CONTRIBUTIONS:

Conceptualization: A. Badaoui. Data curation: R. Kahlouche, M. Criado. Formal analysis: R. Kahlouche, M. Criado. Fund raising: A. Badaoui. Research: R. Kahlouche, M. Criado, A. Badaoui. Methodology: M. Criado, R. Kahlouche, A. Badaoui. Project administration: A. Badaoui. Resources: R. Kahlouche, A. Badaoui. Software: R. Kahlouche. Supervision: M. Criado, A. Badaoui. Validation: M. Criado, A. Badaoui. Visualization: M. Criado, A. Badaoui. Writing original draft: R. Kahlouche. Writing, review & editing: M. Criado, A. Badaoui.

REFERENCES

1. Cadore, D.E.; da Luz, C.A.; de Medeiros, M.F. (2019) An investigation of the carbonation of alkaline activated cement made from blast furnace slag generated by charcoal. *Constr. Build. Mater.* 226, 117-125. https://doi.org/10.1016/j.conbuildmat.2019.07.209.
2. Deja, J.; Uliasz-Bochenczyk, A.; Mokrzycki, E. (2010) CO_2 emissions from Polish cement industry. *Int. J. Greenh. Gas Control.* 4 [4], 583-588. https://doi.org/10.1016/j.ijggc.2010.02.002.
3. Van Deventer, J.S.; Provis, J.L.; Duxson, P. (2012) Technical and commercial progress in the adoption of geopolymer cement. *Miner. Eng.* 29, 89-104. https://doi.org/10.1016/j.mineng.2011.09.009.
4. Haha, M.B.; Lothenbach, B.; Le Saout, G.; Winnefeld, F. (2012) Influence of slag chemistry on the hydration of alkali-activated blast-furnace slag—Part II: Effect of Al_2O_3. *Cem. Concr. Res.* 42 [1], 74-83. https://doi.org/10.1016/j.cemconres.2011.08.005.
5. Wang, S.D.; Scrivener, K.L.; Pratt, P.L. (1994) Factors affecting the strength of alkali-activated slag. *Cem. Concr. Res.* 24 [6], 1033-1043. https://doi.org/10.1016/0008-8846(94)90026-4.
6. Fernández-Jiménez, A.; Puertas, F. (2003) Effect of activator mix on the hydration and strength behaviour of alkali-activated slag cements. *Adv. Cem. Res.* 15 [3], 129-136. https://doi.org/10.1680/adcr.2003.15.3.129.
7. Živica, V. (2007) Effects of type and dosage of alkaline activator and temperature on the properties of alkali-activated slag mixtures. *Constr. Build. Mater.* 21 [7], 1463-1469. https://doi.org/10.1016/j.conbuildmat.2006.07.002.
8. Fernández-Jiménez, A.; Puertas, F. (2001) Setting of alkali-activated slag cement, Influence of activator nature. *Adv. Cem. Res.* 13 [3], 115-121. https://doi.org/10.1680/adcr.2001.13.3.115.
9. Bakharev, T.; Sanjayan, J.G.; Cheng, Y.B. (1999) Alkali activation of Australian slag cements. *Cem. Concr. Res.* 29 [1], 113-120. https://doi.org/10.1016/S0008-8846(98)00170-7.
10. Gebregziabiher, B.S.; Thomas, R.J.; Peethamparan, S. (2016) Temperature and activator effect on early-age reaction kinetics of alkali-activated slag binders. *Constr. Build. Mater.* 113, 783-793. https://doi.org/10.1016/j.conbuildmat.2016.03.098.
11. Krizan, D.; Zivanovic, B. (2002) Effects of dosage and modulus of water glass on early hydration of alkali–slag cements. *Cem. Concr. Res.* 32 [8], 1181-1188. https://doi.org/10.1016/S0008-8846(01)00717-7.
12. Zuo, Y.; Nedeljković, M.; Ye, G. (2019) Pore solution composition of alkali-activated slag/fly ash pastes. *Cem. Concr. Res.* 115, 230-250. https://doi.org/10.1016/j.cemconres.2018.10.010.
13. Palomo, A.; Krivenko, P.; Garcia-Lodeiro, I.; Kavalerova, E.; Maltseva, O.; Fernández-Jiménez, A. (2014) A review on alkaline activation: new analytical perspectives. *Mater. Construcc.* 64 [315], e022. https://doi.org/10.3989/mc.2014.00314.
14. Reddy, K.C.; Subramaniam, K.V. (2020) Blast furnace slag hydration in an alkaline medium: influence of sodium content and sodium hydroxide molarity. *J. Mater. Civ. Eng.* 32 [12], 04020371. https://doi.org/10.1061/(ASCE)MT.1943-5533.0003455.
15. Bai, Y.; Collier, N.C.; Milestone, N.B.; Yang, C.H. (2011) The potential for using slags activated with near neutral salts as immobilisation matrices for nuclear wastes containing reactive metals. *J. Nucl. Mater.* 413 [3], 183-192. https://doi.org/10.1016/j.jnucmat.2011.04.011.
16. Adesina, A.D. (2018) Effect of green activators on the properties of alkali activated materials: a review. *RILEM Publications*. 1, 431-436. https://doi.org/10.5281/zenodo.1405562.
17. Turner, L.K.; Collins, F.G. (2013) Carbon dioxide equivalent (CO2-e) emissions: A comparison between geopolymer and OPC cement concrete. *Constr. Build. Mater.* 43, 125-130. https://doi.org/10.1016/j.conbuildmat.2013.01.023.
18. Palomo, A.; Maltseva, O.; Garcia-Lodeiro, I.; Fernández-Jiménez, A. (2021) Portland Versus Alkaline Cement: Continuity or Clean Break: "A Key Decision for Global Sustainability". *Front. Chem.* 653. https://doi.org/10.3389/fchem.2021.705475.
19. Bakharev, T.; Sanjayan, J.G.; Cheng, Y.B. (2003) Resistance of alkali-activated slag concrete to acid attack. *Cem. Concr. Res.* 33 [10], 1607-1611. https://doi.org/10.1016/S0008-8846(03)00125-X.

20. Baščarevć, Z. (2015) The resistance of alkali-activated cement-based binders to chemical attack, In Handbook of alkali-activated cements, mortars and concretes. *Woodhead Publishing*. 373-396. https://doi.org/10.1533/9781782422884.3.373.
21. Aydın, S.; Baradan, B. (2014) Effect of activator type and content on properties of alkali-activated slag mortars. *Compos. B. Eng.* 57, 166-172. https://doi.org/10.1016/j.compositesb.2013.10.001.
22. Palacios, M.; Puertas, F. (2007). Effect of shrinkage-reducing admixtures on the properties of alkali-activated slag mortars and pastes. *Cem. Concr. Res.* 37 [5], 691-702. https://doi.org/10.1016/j.cemconres.2006.11.021.
23. Hu, X.; Shi, C.; Zhang, Z.; Hu, Z. (2019) Autogenous and drying shrinkage of alkali-activated slag mortars. *J. Am. Ceram. Soc.* 102 [8], 4963-4975. https://doi.org/10.1111/jace.16349.
24. Siad, H.; Mesbah, H.A.; Khelafi, H.; Kamali-Bernard, S.; Mouli, M. (2010) Effect of mineral admixture on resistance to sulphuric and hydrochloric acid attacks in self-compacting concrete. *Can. J. Civ. Eng.* 37 [3], 441-449. https://doi.org/10.1139/L09-157.
25. Aliques-Granero, J.; Tognonvi, T.M.; Tagnit-Hamou, A. (2017) Durability test methods and their application to AAMs: case of sulfuric-acid resistance. *Mater. Struct.* 50 [1], 1-14. https://doi.org/10.1617/s11527-016-0904-7.
26. Thunuguntla, C.S.; Rao, T.G. (2018) Effect of mix design parameters on mechanical and durability properties of alkali activated slag concrete. *Constr. Build. Mater.* 193, 173-188. https://doi.org/10.1016/j.conbuildmat.2018.10.189.
27. Pereira, A.; Akasaki, J.L.; Melges, J.L.; Tashima, M.M.; Soriano, L., Borrachero, M.V.; Monzó, J.; Payá, J. (2015) Mechanical and durability properties of alkali-activated mortar based on sugarcane bagasse ash and blast furnace slag. *Ceram. Int.* 41 [10], 13012-13024. https://doi.org/10.1016/j.ceramint.2015.07.001.
28. Neville, A. (2004) The confused world of sulfate attack on concrete. *Cem. Concr. Res.* 34 [8], 1275-1296. https://doi.org/10.1016/j.cemconres.2004.04.004.
29. Giménez, M.; Alonso, M.C.; Menéndez, E.; Criado, M. (2021) Durability of UHPFRC functionalised with nanoadditives due to synergies in the action of sulphate and chloride in cracked and uncracked states. *Mater. Construcc*. 71 [344], e264. https://doi.org/10.3989/mc.2021.14021.
30. Santillán, L.R.; Locati, F.; Villagrán-Zaccardi, Y.A.; Zega, C.J. (2020) Long-term sulfate attack on recycled aggregate concrete immersed in sodium sulfate solution for 10 years. *Mater. Construcc.* 70 [337], e212. https://doi.org/10.3989/mc.2020.06319.
31. Flatt, R. J.; Scherer, G. W. (2008). Thermodynamics of crystallization stresses in DEF. *Cem. Concr. Res.* 38 [3], 325-336. https://doi.org/10.1016/j.cemconres.2007.10.002.
32. Liu, L.; Xie, M.; He, Y.; Li, Y.; Huang, X.; Cui, X.; Shi, C. (2020) Expansion behavior and microstructure change of alkali-activated slag grouting material in sulfate environment. *Constr. Build. Mater.* 260, 119909. https://doi.org/10.1016/j.conbuildmat.2020.119909.
33. Beltrame, N.A.M.; da Luz, C.A.; Perardt, M.; Hooton, R.D. (2020) Alkali activated cement made from blast furnace slag generated by charcoal: Resistance to attack by sodium and magnesium sulfates. *Constr. Build. Mater.* 238, 117710. https://doi.org/10.1016/j.conbuildmat.2019.117710.
34. Allahvedi, A.; Hashemi, H. (2015) Investigating the resistance of alkali-activated slag mortar exposed to magnesium sulfate attack. *Int. J. Civ. Eng.* 13 [4], 379-387. Retrieved from http://ijce.iust.ac.ir/article-1-907-en.html.
35. Ye, H.; Chen, Z.; Huang, L. (2019). Mechanism of sulfate attack on alkali-activated slag: The role of activator composition. *Cem. Concr. Res.* 125, 105868. https://doi.org/10.1016/j.cemconres.2019.105868.
36. Yang, T.; Gao, X.; Zhang, J.; Zhuang, X.; Wang, H.; Zhang, Z. (2022). Sulphate resistance of one-part geopolymer synthesized by calcium carbide residue-sodium carbonate-activation of slag. *Compos. B. Eng.* 242, 110024. https://doi.org/10.1016/j.compositesb.2022.110024.
37. Kahlouche, R.; Badaoui, A. (2022) Mechanical performance and durability of mortar based on slag cement and NaOH-activated slag. *Mater. Sci. Forum.* 1078, 179-188. https://doi.org/10.4028/p-j578h5.
38. Kiiashko, A.; Chaouche, M.; Frouin, L. (2021) Effect of phosphonate addition on sodium carbonate activated slag properties. *Cem. Concr. Com*. 119, 103986. https://doi.org/10.1016/j.cemconcomp.2021.103986.
39. Jin, F.; Al-Tabbaa, A. (2015) Strength and drying shrinkage of slag paste activated by sodium carbonate and reactive MgO. *Constr. Build. Mater.* 81, 58-65. https://doi.org/10.1016/j.conbuildmat.2015.01.082.
40. Kashani, A.; Provis, J.L.; Qiao, G.G.; van Deventer, J.S. (2014) The interrelationship between surface chemistry and rheology in alkali activated slag paste. *Constr. Build. Mater.* 65, 583-591. https://doi.org/10.1016/j.conbuildmat.2014.04.127.
41. Palacios, M.; Gismera, S.; Alonso, M.D.M.; de Lacaillerie, J.D.E.; Lothenbach, B.; Favier, A.; Brumaud, C.; Puertas, F. (2021) Early reactivity of sodium silicate-activated slag pastes and its impact on rheological properties. *Cem. Concr. Res.* 140, 106302. https://doi.org/10.1016/j.cemconres.2020.106302.
42. Criado, M.; Fernández-Jiménez, A.; Palomo, A.; Sobrados, I.; Sanz, J. (2008) Effect of the SiO_2/Na_2O ratio on the alkali activation of fly ash. Part II: 29Si MAS-NMR Survey. *Microp. Mesop.* 109 [1-3], 525-534. https://doi.org/10.1016/j.micromeso.2007.05.062.
43. Awoyera, P.; Adesina, A. (2019) A critical review on application of alkali activated slag as a sustainable composite binder. *Case Stud. Constr. Mater.* 11, e00268. https://doi.org/10.1016/j.cscm.2019.e00268.
44. Puertas, F.; Varga, C.; Alonso, M.M. (2014) Rheology of alkali-activated slag pastes. Effect of the nature and concentration of the activating solution. *Cem. Concr. Compos.* 53, 279-288. https://doi.org/10.1016/j.cemconcomp.2014.07.012.
45. Bernal, S.A.; Provis, J.L.; Myers, R.J.; San Nicolas, R.; van Deventer, J.S. (2015) Role of carbonates in the chemical evolution of sodium carbonate-activated slag binders. *Mater. Struct.* 48 [3], 517-529. https://doi.org/10.1617/s11527-014-0412-6.
46. Yuan, B.; Yu, Q.L.; Brouwers, H.J.H. (2017) Time-dependent characterization of Na_2CO_3 activated slag. *Cem. Concr. Compos.* 84, 188-197. https://doi.org/10.1016/j.cemconcomp.2017.09.005.
47. Kovtun, M.; Kearsley, E.P.; Shekhovtsova, J. (2015) Chemical acceleration of a neutral granulated blast-furnace slag activated by sodium carbonate. *Cem. Concr. Res.* 72, 1-9. https://doi.org/10.1016/j.cemconres.2015.02.014.
48. Lahalle, H.; Benavent, V.; Trincal, V.; Wattez, T.; Bucher, R.; Cyr, M. (2021) Robustness to water and temperature, and activation energies of metakaolin-based geopolymer and alkali-activated slag binders. *Constr. Build. Mater.* 300, 124066. https://doi.org/10.1016/j.conbuildmat.2021.124066.
49. Scherer, G.W. (2015) Drying, shrinkage, and cracking of cementitious materials. *Transp. Poro. Media.* 110, 311-331. https://doi.org/10.1007/s11242-015-0518-5.
50. Collins, F.; Sanjayan, J.G. (2000) Effect of pore size distribution on drying shrinking of alkali-activated slag concrete. *Cem. Concr. Res.* 30 [9], 1401-1406. https://doi.org/10.1016/S0008-8846(00)00327-6.
51. Wang, S.D.; Pu, X.C.; Scrivener, K.L.; Pratt, P.L. (1995) Alkali-activated slag cement and concrete: a review of properties and problems. *Adv. Cem. Res.* 7 [27], 93-102. https://doi.org/10.1680/adcr.1995.7.27.93.
52. Li, J.; Yu, Q.; Huang, H.; Yin, S. (2019) Difference in the reaction process of slag activated by waterglass solution and NaOH solution. *Struct. Concr.* 20 [5], 1528-1540. https://doi.org/10.1002/suco.201900130.
53. Adesina, A. (2021) Performance and sustainability overview of sodium carbonate activated slag materials cured at ambient temperature. *Resour. Environ. Sustain.* 3, 100016. https://doi.org/10.1016/j.resenv.2021.100016.
54. Ayub, T.; Shafiq, N.; Khan, S. (2013) Durability of concrete with different mineral admixtures: A comparative review. *World Acad. Sci. Engineer. Technol. Int. J. Civ. Eng.* 7 [8], 1161-1172.
55. Komljenović, M.; Baščarević, Z.; Marjanović, N.; Nikolić, V. (2013) External sulfate attack on alkali-activated slag. *Constr. Build. Mater.* 49, 31-39. https://doi.org/10.1016/j.conbuildmat.2013.08.013.

56. Aliques-Granero, J.; Tognonvi, M.T.; Tagnit-Hamou, A. (2019) Durability study of AAMs: Sulfate attack resistance. *Constr. Build. Mater.* 229, 117100. https://doi.org/10.1016/j.conbuildmat.2019.117100.

57. de Hita, M.J.; Criado, M. (2023). Influence of superplasticizers on the workability and mechanical development of binary and ternary blended cement and alkali-activated cement. *Constr. Build. Mater.* 366, 130272. https://doi.org/10.1016/j.conbuildmat.2022.130272.